Multi-Scale Modeling of Human Cornea

BY

DIPIKA GONGAL
B.S., Tribhuvan University, 2008

THESIS

Submitted as partial fulfillment of the requirements
for the degree of Master of Science in Civil Engineering
in the Graduate College of the
University of Illinois at Chicago, 2012

Chicago, Illinois

Defense Committee:

Craig Foster, Chair and Advisor
Didem Ozevin
Ahmed A. Shabana, Mechanical and Industrial Engineering

ACKNOWLEDGEMENT

I would like to express my deep gratitude to my advisor, Professor Craig Foster, for his constant support, encouragement and guidance from the initial to the final stage of my work. This thesis would not have been completed without his teaching of the subject. I could not have imagined a better advisor and a mentor.

I am also grateful for my thesis committee Professor Ahmed A. Shabana and Professor Didem Ozevin for their valuable comments and time. I would also like to thank my colleagues Ahmed El-Ghandour, David Weed and Talisa Mohammad Nejad for their help and providing me a fun learning environment. I would also like to thank my summer research teams for their contributions to the research work.

Finally, I would like to thank my friend, Manish Shrestha and my family members for their motivation and encouragement to complete this work.

TABLE OF CONTENTS

LIST OF FIGURES iv
LIST OF TABLES v
SUMMARY vi

CHAPTER 1 1

1.1 Objective 1

1.2 Introduction 3

CHAPTER 2 6

2.1 Study of Individual Collagen fibril and Cornea strips 6

2.2 Mechanical Properties of Collagen 6
2.2.1 Modeling of collagen fibril 8
2.2.2 Results 10

2.3 Modeling of Corneal Tissue 12
2.3.1 Methodology 12
2.3.2 Material model 15
2.3.3 Geometric model 19
2.3.4 Review of experiments of corneal stiffness 19
2.3.5 Results and Comments 21

CHAPTER 3 23

3.1 Finite Element Modeling of Human Cornea 23

3.2 Mechanical Properties of Cornea 24

3.3 Modeling of Human Cornea 24
3.3.1 Material model 26
3.3.2 Geometric model 30

3.4 Results and Comment 32

CHAPTER 4 38

4.1 Comments and Conclusion 38

LIST OF REFERENCES 41

VITA 43

LIST OF FIGURES

Figure 1: Schematic view of hierarchical features of collagen structure 3

Figure 2: D-staggered arrangement of the collagen fibrils showing the cross-links between the tropocollagen molecules 4

Figure 3: Typical stress-strain curve of collagen fibril showing different regions under uniaxial tensile loading. 7

Figure 4 : Schematic diagram of model from Albanese *et al (*2009) 9

Figure 5 : Stress-strain curve of collagen fibril for exponential, two elastic element and new model compared with experimental data from Van der Rijt *et al* (2006) 10

Figure 6: Collagen fibril distribution in the cornea in two preferred orientation. 16

Figure 7: Cube element deformed under tensile pressure on one side and fixed on the other end. 19

Figure 8: Stress-strain graph fit for the new model. 21

Figure 9: Displacement boundary condition and pressure loading applied in cornea model 25

Figure 10: 3-Dimensional finite element model showing the dimensions of the cornea. The outer diameter of the cornea is 11.61mm with thickness of 627 μm at the center and 756 μm at the limbus. The maximum elevation at the apex is 2.52mm. 30

Figure 11: Top view, side view and general view of the 2340 elements meshed human cornea. 31

Figure 12: Pressure-Displacement profile for the human cornea 32

Figure 13: Stress versus pressure for 1170 and 2340 mesh elements showing the convergence of the stress values. 33

Figure 14: Non-linear response obtained for the cornea model at high IOP 34

Figure 15: Displacement mapping of the human cornea at 18 mmHg IOP 34

Figure 16: Cross-sectional view of displacement in the cornea. The solid figure shows the original structure and the wired mesh figure shows the deformed shape of the corneal due to 18 mmHg of pressure. 35

Figure 17: Stress mapping of the cornea. 36

Figure 18: Spiral pattern obtained for the cornea model for maximum in plane shear 36

LIST OF TABLES

Table 1: Parameters obtained from least square method..... 11

Table 2: Parameter values for the cornea strip model. 18

Table 3: Parameter values for the cornea model 29

SUMMARY

The human cornea is the medium through which vision is possible. Any kind of defect to the cornea affects the vision of a person, hampering the quality of life. Studies regarding human cornea is necessary to understand the problems and treatments to normalize the defects. This study was performed to understand the biomechanical response of the human cornea by using the structural analysis tool. The cornea response was studied in three hierarchial levesl: i) fibril; ii) tissue; and iii) entire cornea. The multi-scale modeling provides a co-relation of the biomechanical response of all the levels of cornea for the better understanding of the response.

Mathematical models of the collagen fibril and cornea tissue were prepared based on the experimental data obtained from the laboratory tests. The models were able to depict the true physiological response under uniaxial tension.

A finite element model of healthy cornea was developed and the analysis results were compared with the experimental results to verify the result. The model was able to reproduce the exact response under the physiological intra-ocular pressure.

The cornea model created can be used to study the response of keratoconus, a disease caused by the loss of cornea tissue stiffness, and cornea cross-linking, a procedure used for the correction of the disease.

CHAPTER 1

1.1 Objective

The cornea is the transparent part of the eye which gives shape to the eye. It covers iris, pupil and anterior chamber of the eye. The cornea refracts light to the lens, which makes vision possible. It is transparent in nature, making it possible for light to travel through it. The curvature and thickness of cornea plays an important role in focusing light to the lens and hence responsible for its optic power (Albanese *et al* 2009). Any kind of adjustment or deformation can result in refractive error and consequently degrading the visual performance of the eye.

The refractive error can lead to defective vision like myopia, hyperopia and astigmatism, to name a few. Myopia (short-sightedness) is the inability of the eye to focus on distant objects, hyperopia (far-sightedness) to focus near objects and astigmatism is the formation of distorted image caused by cornea surface irregularities. These defects can be treated by different types of refractive surgeries. Laser in situ keratomileusis (LASIK), Photorefractive Keratectomy (PRK), and Arcuate Keratotomy (AK) techniques are some popular refractive surgery, which involves optimizing the curvature to obtain correct vision (Alastrué *et al* 2006).

Keratoconus is a progressive degenerative eye disease caused by the degradation of the biomechanical properties of the cornea material (Andreasse *et al* 1980). It is estimated to affects 1 in 2000 individuals (Rabinowitz *et al* 1998). The exact cause of the disease has not been identified yet. It causes localized thinning up to 75% thickness (Bron *et al* 1988, Edmund *et al* 1989) of the cornea causing bulging of the affected area and creating irregular cornea surface. It can be temporarily corrected by the use of glasses or hard contact lenses and ocular transplant. As the disease progress and gets severe corneal transplant may be required.

Biomechanical procedures can also used to stabilize the corneal strength. Corneal cross-linking is one kind of biomechanical procedure for permanent treatment of keratoconus. In this treatment cornea is treated by applying riboflavin solution followed by cornea exposure to UVA radiation (Raiskup Wolf *et al* 2008). The treatment increases the cross-link density and strengthens the cornea.

These treatment techniques are fairly effective in treating or preventing the progression of the disease. However, the outcomes may not be as expected and vary from patient to patient. The treatment involving the alteration of cornea shape and material is highly risky as it affects both the structural and mechanical properties in an unpredicted manner. Research involving biomechanical modeling of the cornea has been used to predict the result of the structural alteration with a certain level of success. However, the effective procedure to treat the defects can only be attained by completely understanding the biological and structural response of the cornea. In depth understanding of the biomechanical response can aid in development of better clinical procedures to minimize post surgery complications.

The objective of the study is to understand the global biomechanical response of the cornea. For this reason, multi-scale study has been carried out for the three levels of cornea material .

1) Fibril Level: Mechanical response study of collagen fibrils investigating the tensile mechanical property.

2) Tissue Level: Mechanical response of collagen tissue under uniaxial tensile load.

3) Whole cornea: Finite element simulation of the numerical model of entire cornea under varying Intra-Ocular pressure.

Research has been carried out on the basis of the fundamental properties of the collagen fibril. The mechanical properties from fibril level to the entire cornea have been studied to correlate the properties of individual collagen fibril with the cornea tissue. Simulation of model is performed using Finite Element Analysis to replicate the natural behavior of the cornea under physiological pressure to understand the response of the cornea.

1.2 Introduction

The mammalian cornea consists of five layers: the epithelium, the Bowman's membrane, the stroma, Descemet's membrane and the endothelium (Pandolfi *et al* 2008), with a total thickness of 0.5–0.6 mm at the center and 0.6–0.8 mm at the periphery where it fuses with the sclera at limbus. Of the five layers, the middle layer, the stroma, makes 90% of the cornea thickness and is the major layer contributing to the mechanical strength and stiffness of the cornea (Maurice 1957).

The stroma is a composite material consisting of matrix embedded with a complex network of collagen fibers throughout the cornea. The matrix is viscoelastic material composed of proteoglycans, glycoproteins and keratocytes (Pandolfi *et al* 2008). This matrix is nearly incompressible in nature and is considered as Neo-Hookean material for the computational purpose.

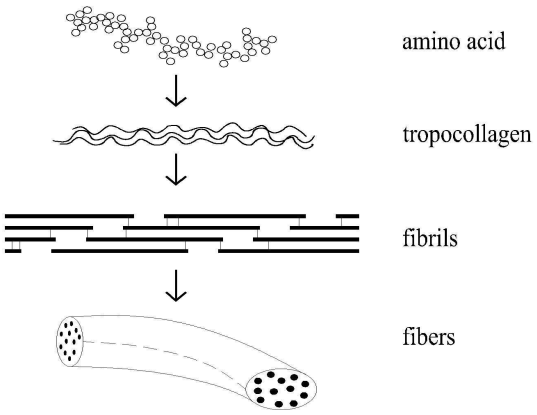

Figure 1: Schematic view of hierarchical features of collagen structure

The collagen fibrils found in stroma layer are of Type I, III, V and VI (Pinsky *et al* 2005). Majority of the collagen fibrils are Type I and are responsible in providing mechanical and elastic property to the tissue. The basic unit of Type I collagen consist of polypeptide chains of amino acids wound into triple helix called tropocollagen having diameter of 1.5nm and length up to 300nm (Kadler *et al* 1996). These tropocollagen molecules cross-link to form collagen fibrils. The cross-linking occurs between tropocollagen as a result of a unique mechanism based on aldehyde formation from lysine or hydroxylysine side chains with the aid of the enzyme lysyl oxidase (Eyre et al 1984). These cross-links prevent relative motion along the fibril axis upon stretching. The collagen fibrils are arranged in the D-staggered manner with an axial periodicity of 67 μm (Graham *et al* 2004) as shown in Figure 2.

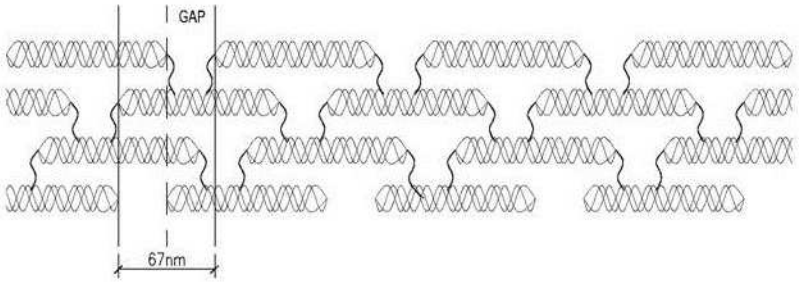

Figure 2: D-staggered arrangement of the collagen fibrils showing the cross-links between the tropocollagen molecules

The fibrils are bundled together to form fibers of thickness 4nm (Graham *et al* 2004). In the cornea, the fibers are stacked parallel to form layers called lamellae of approximate thickness 1.5-2.5μm (Alastrué *et al* 2006). The stroma consists of about 300 lamella stacked through the thickness at the center of the cornea and about 500 at the limbus (Pinsky *et al* 2005).

The fibers act as reinforcement to the tissue and give mechanical strength along the axial direction. The arrangements of collagen fibrils are important to determine the mechanical

strength of the cornea. X-ray scatter intensity distribution indicated two preferred directions of collagen orientation, Nasal-Temporal and Superior-Inferior at the center of the cornea. At limbus they tend to run in the circumferential direction and eventually fuse with sclera (Meek and Newton 1999). The preferred direction is found to be more prevalent in the posterior half of the cornea (Pinsky *et al* 2005). The preferred orientation of the fibrils is about 66% and the remaining 33% has random orientation (Daxer and Fratzl 1997, Pandolfi *et al* 2005). This arrangement of the collagen fibrils results in anisotropy of the cornea material.

CHAPTER 2

2.1 Study of Individual Collagen Fibrils and Cornea Strips

For understanding the characteristics of human cornea it becomes necessary to understand the biomechanical response of its constituents. The collagen fibril is an integral part of the cornea and acts as a backbone to provide cornea with its mechanical strength. The response of the collagen fibril was studied to build a stress and strain response relationship. The established relationship was used to study the mechanical response of the corneal strips or tissue. The relationship between stress and strain of the collagen fibril was then used to model an entire cornea.

The study of collagen fibril and its influence to the mechanical strength is very important in describing the mechanical properties of cornea. During keratoconus, the stiffness provided by the linked fibers degrades. The fibril orientation in the affected area is also disturbed decreasing the tissue stiffness (Carvalho *et al* 2009). The corneal cross-linking procedure for the treatment of the keratoconus increases the number of cross-links in the fibrils and restores the strength to the cornea (Raiskup-Wolf *et al* 2008). For the evaluation of the keratoconus and its treatment, assessment of the changes of stress in the fibril thus becomes necessary.

2.2 Mechanical Properties of Collagen

Collagen is a fibrous structural protein abundantly found in biological tissues of vertebrate and invertebrate species, including bone, tendon, teeth, cartilage, the cornea and the cardiovascular system. The primary function of the collagen is to provide rigidity and to strengthen the tissue. The fibrils in the tissue are the major contributor of overall mechanical strength of the tissue. They act as reinforcement and resist against deformation. Under physiological conditions they are elastically stretched and by natural condition do not take any

compressive force (Pandolfi *et al* 2008). The mechanical response of the collagen tissue can be understood by studying the characteristics of the collagen fibrils which are dispersed in the collagen.

The typical stress-strain curve of a collagen fibril under tensile load is shown in Figure 3. The graph shows three distinct regions under deformation. These different regions mark major structural changes in the fibril while undergoing deformation. Region 1 is characterized by unwinding of the helical structure of the fibril and can be approximated as a linear region. As the collagen fibril unwinds it starts to straighten and becomes stiffer. Sudden stiffening causes steep increase in the stress which is the characteristic behavior of Region 2. This region is marked by stretching of polypeptide backbone causing sliding of fibrils with respect to each others. Further increase in stress leads to stretching of the fibrils marked as Region 3. In the figure, ε_u marks the end of unwinding and ε_s marks the beginning of the stretching regime.

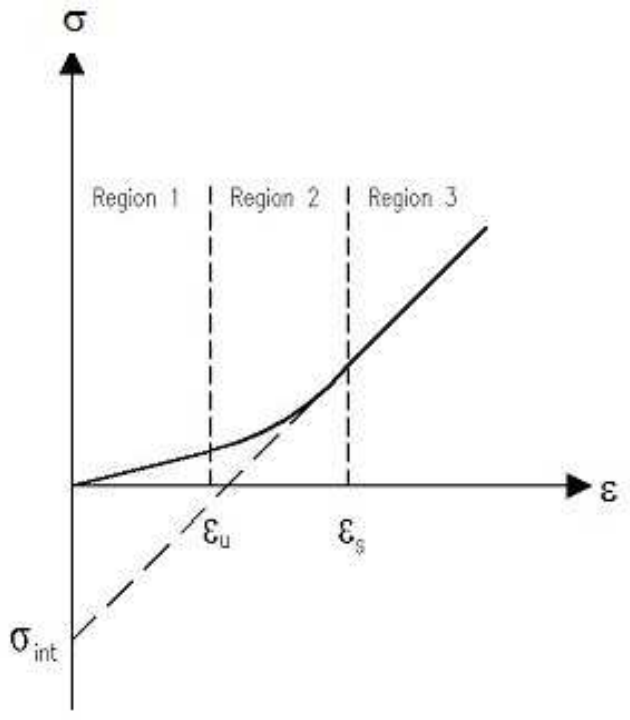

Figure 3: Typical stress-strain curve of collagen fibril showing different regions under uniaxial tensile loading.

Several articles were reviewed to understand the biomechanical property of collagen fibril. A brief literature review of some notable papers is presented below.

Grahams *et al* (2004) tested type I collagen fibrils under tensile loading and determined the Young's Modulus to be 32 Mpa at about 4% strain. The force versus displacement graph was unsmooth with several peaks and drops between the force range of 1.5 - 4.5 nN. The discontinuity observed, indicates major structural reorganization within the fibrillar structure.

Van der Rijt *et al* (2006) tested individual collagen fibrils in ambient condition up to its elastic limit of 90 Mpa with resulting Young's Modulus to be 2 ~ 7 Gpa. In aqueous medium, the fibrils stretched elastically up to the stress of 15 Mpa at 4% stain with resulting Young's Modulus of 0.2 ~ 0.8 Gpa.

Buehler *et al* (2008) carried out multi-scale modeling, comparing the tropocollagen molecule with the collagen fibrils at varying cross-link densities. Results showed that the increase in cross-link density increased its stiffness and made the fibrils brittle.

Sevensson *et al* (2010) showed the dependence of the strain rate on tensile tests of the collagen fibril. He showed the increase in strain rate caused stiffer response of the fibril by testing collagen at six different strain rates. The non-linear response observed was similar to the result obtained from the Van der Rijt *et al* (2006). It should be noted that in this thesis we will ignore the viscous effects of the materials, focusing on the non-linear elastic behavior.

2.2.1 Modeling of collagen fibril

The stress-strain relationship of individual collagen fibril is expressed phenomenologically by an exponential equation

$$\sigma_{exponential} = a(e^{b\varepsilon} - 1) \qquad (1)$$

where *a* and *b* are the coefficient parameters which are determined by fitting to the experimental data. σ and ε are the nominal stress and small strain.

The collagen fibril mechanical characteristic was tried to explain by Albanese *et al* (2009) using a two elastic element model which included a longitudinal spring and a transverse spring with one shared fixed end and the other ends attached to non-deformable set-square that can slide in the longitudinal direction as shown in Figure 4. The equation formulated to describe the mechanical response of fibril is

$$\sigma_{elastic\_elements} = E_L\varepsilon + kE_T\varepsilon(1-\frac{1}{\sqrt{1+k^2\varepsilon^2}}) \qquad (2)$$

E_L is the modulus of the longitudinal spring, E_T is the modulus of the transverse spring, and *k* is the coefficient describing the ratios of the set–square.

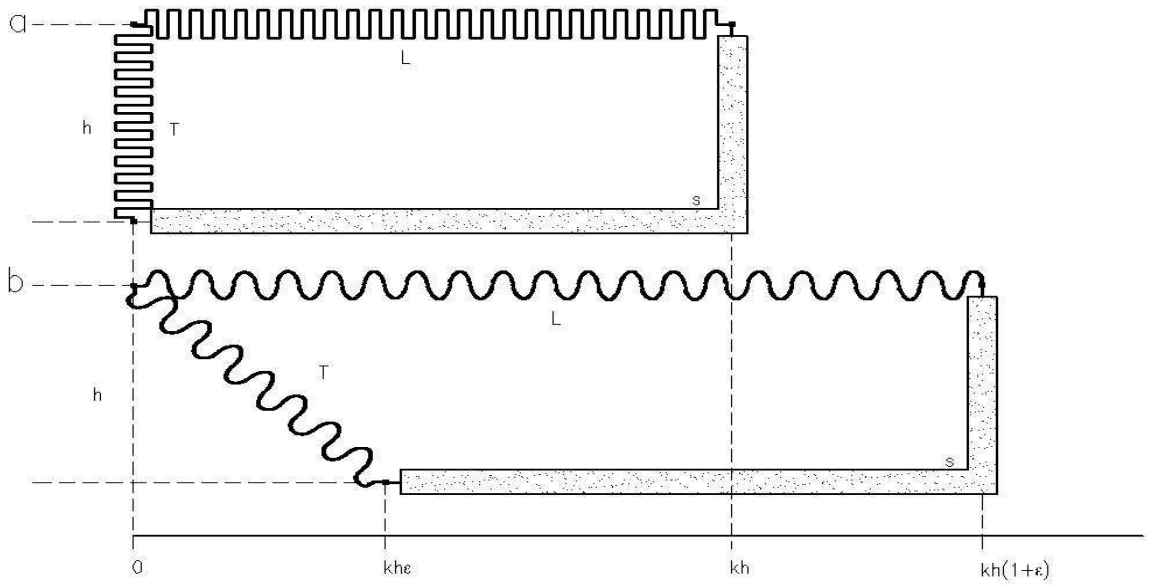

Figure 4 : Schematic diagram of model from Albanese *et al (*2009)

The Exponential and Albanese models are based on the general mechanical characteristic of the collagen fibril under the applied load. A new model has been formulated to better account for the true physiological response under tensile load give by

$$\sigma_f(\varepsilon) = \begin{cases} \beta E_u \varepsilon & \varepsilon < \varepsilon_u \\ \beta E_u \varepsilon + \beta \dfrac{(E_u - E_s)(\varepsilon - \varepsilon_u)^2}{2(\varepsilon_s - \varepsilon_u)} & \varepsilon_u < \varepsilon < \varepsilon_s \\ \beta[E_s \varepsilon - \sigma_{\text{int}}] & \varepsilon > \varepsilon_s \end{cases} \quad (3)$$

where β is the cross-linking density, E_u is the modulus of the unwinding regime, E_s is the modulus of the stretching regime, ε_u is the strain where the unwinding regime ends, ε_s is the strain where the stretching regime begins and σ_{int} is the y-intercept of the linear stretching regime.

2.2.2 Results

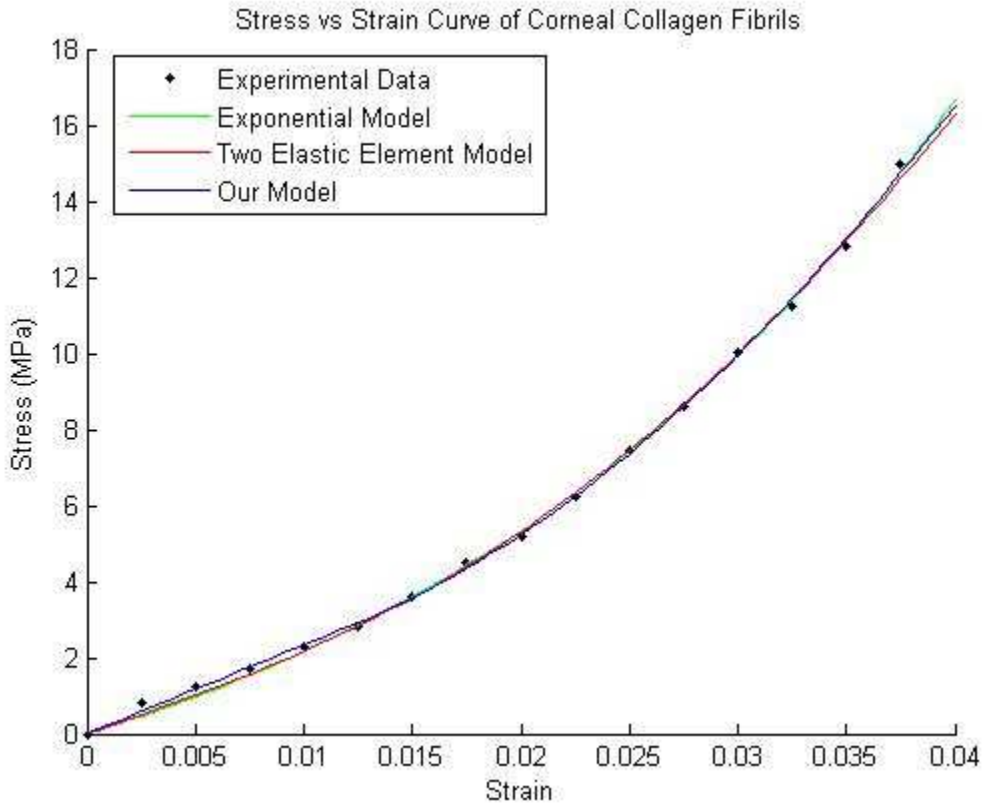

Figure 5 : Stress-strain curve of collagen fibril for exponential, two elastic element and new model compared with experimental data from Van der Rijt *et al* (2006)

The equations formulated to define the stress-strain relationship of the collagen fibril given by Equations (1), (2) and (3) were fitted with the experimental data to determine the values for the parameters. The experimental data obtained from Van der Rijt *et al* (2006) for collagen fibrils tested under aqueous medium was used to fit the equations. The stress-strain curve obtained for the models is shown in Figure 5

Least square regression method was applied to fit the equations with the experimental data. The values of the parameter were determined and errors for each equation were calculated. The new model fitted the best with error R^2 value 0.9992. The R^2 value of exponential model and two elastic elements model were 0.9988 and 0.9986 respectively. The values for the three models obtained after parameter fitting are given in Table 1.

Table 1: Parameters obtained from least square method

Model	**Parameter**	**Values**	**Error, R^2**
Exponential Model	a b	4.7273 Mpa 0.3776	0.9988
Two Elastic Element Model	E_L E_T K	1.9870 Mpa 52.8120 Mpa 0.1916	0.9986
New Model	E_u E_s ε_u ε_s β	2.340 Mpa 7.0967 Mpa 1.230% 3.761% 1	0.9992

After fitting the parameters we can conclude that the equations successfully depict the mechanical characteristics of the collagen fibril under tensile loading. The models created for the collagen fibrils shall now be used to determine the mechanical characteristics of the collagen tissue.

2.3 Modeling of Cornea Tissue

Corneal tissue is a soft biological material. It is nearly incompressible in nature and possesses non-linear elastic behavior. It undergoes large deformation under application of load and upon removal of load return back to its original shape. Such characteristics of corneal tissue become the basis upon which the model will be created.

The corneal tissue is composed of a matrix and collagen fibrils. The biomechanical response shown by the tissue is due to the characteristics of its components. Thus a model of the corneal tissue will be based on the characteristic of extracellular matrix and collagen fibril. The models created for the collagen fibrils will be tested to see if it can reproduce the mechanical characteristics of the tissue. The results from the analysis will be compared with the laboratory data to validate the model. The model which satisfies the corneal tissue characteristics will be represented in the modeling for entire cornea.

2.3.1 Methodology

The approach behind creating a model for corneal tissue material is by applying mathematical functions that depicts the true physiological response of the tissue. The equations formulated for collagen fibrils and a constitutive model for extracellular matrix are combined together to define the tissue material. Using the model, simulations for the uniaxial test are performed by implementing finite element analysis method. The analysis was carried out in Total Lagrangian system, using the material coordinate system. The stress and strain measures used are Second Piola-Kirchhoff stress tensor and Right Cauchy-Green deformation tensor.

The model developed was used to predict the stress under the given strain. For the initial calculation displacement was assumed and strain and stresses values were determined. The calculated stress values give the internal force ($\boldsymbol{f}^{int}$) of the system. The calculated internal force

was compared with the external force ($\boldsymbol{f}^{ext}$) to determine whether the condition of equilibrium is satisfied. The external force is computed from the external load applied to the system. In our case we apply uniformly distributed pressure over one surface. To satisfy the equilibrium condition, the internal force must be equal to the external force. The difference between internal and external force is calculated as shown in equation (4).

$$\boldsymbol{r} = \left| \boldsymbol{f}^{int} - \boldsymbol{f}^{ext} \right| \tag{4}$$

where r is the residual of the forces and is expected to be near zero. If r is larger than zero than Newton-Raphson Iteration method is applied until the value of r is less than a small tolerance value. The finite element coding algorithm is given below:

Box 1: General Algorithm for the finite element analysis

(1) Input mesh, boundary conditions, material properties, time step (Δt), final time (t_f) and tolerance.

(2) Calculate element shape function, initial gradient of shape function and Jacobian of all elements.

(3) Assume displacement $\boldsymbol{d} = \boldsymbol{d_0}$ (usually $\mathbf{0}$) and $t = 0$.

(4) $t = t + \Delta t$

(5) while $t < t_f$

i. loop over elements, calculate $\boldsymbol{f}^{int}$ and $\boldsymbol{f}^{ext}$ for all elements

ii. Assemble forces

iii. Calculate residual for initial guess, $\boldsymbol{r_0} = \boldsymbol{f}^{ext} - \boldsymbol{f}^{int}$

iv. while $||\boldsymbol{r}|| / ||\boldsymbol{r_0}|| >$ tolerance

a) calculate displacement, $\boldsymbol{d} = \boldsymbol{d} + [\mathrm{d}(\boldsymbol{f}^{int})/ \mathrm{d}(\boldsymbol{d})]^{-1} * \boldsymbol{r}$

b) loop over elements, calculate new $\boldsymbol{f}^{int}$

c) assemble internal force

d) calculate new residual

v. $t = t + \Delta t$

vi. if step 5 fails

a) $t = t - \Delta t$

b) $\Delta t = \Delta t/2$

c) Return to step 4

(6) Update, output variables (displacement, stress, and strain)

The computation of the stresses and strain were used to determine the internal force. The sub-function for the calculation of the internal force is described in Box 2.

Box 2: Sub-function for the calculation of internal force

(1) compute the measures of deformation

a) Deformation gradient (***F***)

b) Green Lagrangian Deformation tensor (***C***)

(2) calculate Second Piola-Kirchhoff stress from the deformation tensor

(3) compute the measures of deformation

$$\boldsymbol{f}^{int} = \int_{\Omega_0} \hat{\boldsymbol{B}}^T \boldsymbol{S} d\Omega_0$$

where $\hat{\boldsymbol{B}}$ is the strain-displacement matrix for the Total Lagrangian formulation and ***S*** is the Second Piola-Kirchhoff stress, J is the jacobian and Ω_0 is the domain in the undeformed configuration.

2.3.2 Material Model

The corneal tissue model is based on the model developed for individual collagen fibrils and extrafibrillary matrix. The response of the tissue is determined by using strain energy density function (Ψ_{total}) which is the sum of strain energy due to matrix (Ψ_{matrix}) and product of strain energy due to fibril (Ψ_{total}) and its angular density function. The angular probability density function gives the directional distribution of the collagen fibril distributed over the corneal strip. The total strain energy density of the corneal strip can expressed by Pinsky *et al* (2005) as follows

$$\Psi_{total} = \Psi_{matrix} + \frac{1}{\pi}\int_0^{\pi} \hat{\phi}(X,Y;\theta)\Psi_{fibril}(X,Y;\theta)d\theta \qquad (5)$$

The total stress developed in the cornea tissue developed from above equation can be expressed as

$$\boldsymbol{S}_{total} = \boldsymbol{S}_{matrix} + \frac{1}{\pi}\int_0^{\pi} \hat{\phi}(X,Y;\theta)\boldsymbol{S}_{fibril}(\boldsymbol{M}\otimes\boldsymbol{M})d\theta \qquad (6)$$

2.3.2.1 Collagen fibril

For the calculation of the strain energy density of fibrils, their orientation must be taken into consideration. The angular probability density function $\hat{\phi}(X,Y;\theta)$ was adopted to describe the fibril orientation, proposed by Pinsky *et al* (2005). The probability density function is based on the x-ray scattering data, which gives probability of fibril orientation at any point (X, Y) making an angle θ with the x-axis along the orientation given by the unit vector $\boldsymbol{M}$. The fibril strain energy density multiplied by the density function gives the total strain energy of the orientated fibril. The density function is expressed in polar coordinate system as defined by Pinsky *et al* (2005)

$$\begin{aligned} \phi(R,\varphi;\theta) &= \cos^{2n}(\theta) + \sin^{2n}(\theta) + c_1 \qquad 0 \le R \le 4 \\ \phi(R,\varphi;\theta) &= \sin^{2n}(\theta - \varphi) + c_2 \qquad 5.5 \le R \le 6.5 \end{aligned} \tag{7}$$

where $\phi(R,\varphi;\theta)$ is the expression of probability density function in the polar coordinate system.

The two equations represent the orthogonal and tangential orientation of the collagen fibrils, which is governed by the radius, *R*. This model was originally developed for the entire cornea and the *R* term is measured from the corneal axis passing through the apex or center of the cornea. Radius less than 4mm represents the central part of cornea where the fibril orientation is in nasal-temporal and inferior-superior direction. The orientation around the circumference of the cornea is in tangential and radial direction, defined in the range of 5.5 and 6.5mm. The orientation between the radius 4 and 5.5mm is taken as the transition from orthogonal to radial-tangential direction. Figure 6 shows the approximate orientation of the collagen fibril in the cornea. Since our model is for the central cornea tissue, the radius is always less than 4mm in this chapter. Hence, the first equation is sufficient to predict the stress strain response.

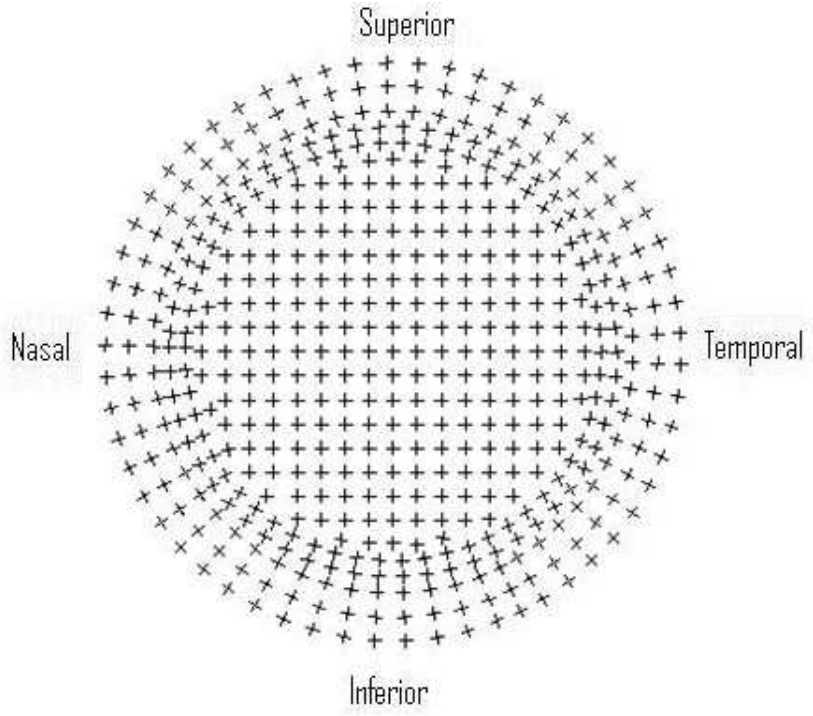

Figure 6: Collagen fibril distribution in the cornea in two preferred orientation.

The constants c_1 and c_2 are found by normalizing the distribution function as shown below

$$\frac{1}{\pi}\int_0^{\pi}\phi(R,\varphi;\theta)d\theta = 1 \tag{8}$$

The exponential constant n was evaluated by fitting to the x-ray scattering data. The values of the parameters used for the Pinsky model is given in Table 2.

The stress due to fibrils $\boldsymbol{S}_{fibril}$ is evaluated by using the individual collagen fibril models: exponential, two elastic element and new model as described by the Equations (1), (2), and (3) respectively. Since these equations are in single degree of freedom, they were transformed to the three degree of freedom by appropriate mathematical manipulation. The Right Cauchy-Green deformation tensor was transformed to small strain ε by introducing stretch parameter as shown below

$$\varepsilon = \lambda - 1 = (\boldsymbol{M}'\boldsymbol{C}\boldsymbol{M})^{1/2} - 1 \tag{9}$$

where λ is the stretch parameter, $\boldsymbol{C}$ is the deformation tensor and $\boldsymbol{M}$ is the fibril orientation vector. The fibril orientation vector is represented as

$$\boldsymbol{M} = \begin{bmatrix} \cos\theta \\ \sin\theta \\ 0 \end{bmatrix} \tag{10}$$

The stress obtained from the calculation is the First Piola-Kirchhoff stress ($\boldsymbol{P}$). The Second Piola-Kirchhoff stress can now be expressed as $\boldsymbol{S} = \boldsymbol{F}^{-1}\boldsymbol{P}$, where $\boldsymbol{F}$ is the deformation gradient. For the uniaxial test, deformation gradient can be expressed by the stretch along the fibril direction. The total stress is then obtained by integrating the stress term with the probability density function, as shown in Equation (6).

2.3.2.2 Collagen matrix

The collagen matrix is nearly incompressible fluid material with low viscosity. The strain energy density of Neo-Hookean model describes these characteristics and is expressed in terms of Cauchy-Green deformation tensor (***C***) as

$$\Psi_{fibril}(\boldsymbol{C}) = \frac{1}{2}\lambda(\ln J)^2 - \mu \ln J + \frac{1}{2}\mu(tr(\boldsymbol{C}) - 3) \tag{11}$$

where λ and μ are bulk and shear modulus also referred as Lame's constants. The Right Cauchy-Green deformation tensor, $\boldsymbol{C} = \boldsymbol{F}^{\mathrm{T}}\boldsymbol{F}$ is the second order symmetric tensor and it satisfies material frame indifference.

The Second Piola-Kirchhoff stress tensor (***S***) can be obtained from strain energy function as shown in Equation (12). The stress tensor is symmetric in nature and also satisfies material frame indifference.

$$\begin{aligned} \boldsymbol{S}_{matrix}(\boldsymbol{C}) &= 2\frac{\partial \Psi}{\partial \boldsymbol{C}} \\ \boldsymbol{S}_{matrix} &= \mu(1 - \boldsymbol{C}^{-1}) + \lambda \ln J\boldsymbol{C}^{-1} \end{aligned} \tag{12}$$

The values of the parameters for collagen fibril were adopted from Pinsky *et al* (2005) and that for extrafibrillary matrix is adopted from Pandolfi *et al* (2008). The values are shown in Table 2.

Table 2: Parameter values for the cornea strip model.

Parameter	λ	μ	c_1	c_2	n
Value	5500 Kpa	60 Kpa	0.45	0.72	4

2.3.3 Geometric model

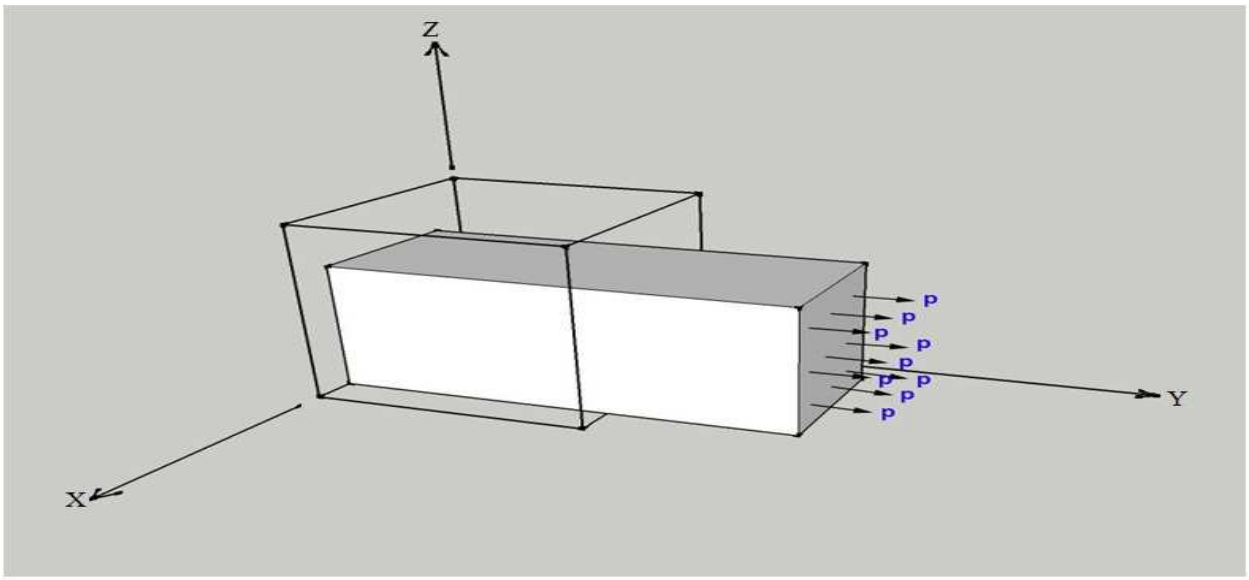

Figure 7: Cube element deformed under tensile pressure on one side and fixed on the other end.

A simple cube element was created for the analysis. The 3-D element was fixed on the left end and pressure was applied on the right end along the positive x-axis as shown in Figure 7. The displacement boundary was set up in such a manner that it allowed both lateral and longitudinal displacements.

2.3.4 Review of experiments of corneal tissue stiffness

The behavior of the corneal tissue has been studied in the laboratory by performing tensile tests on the tissue specimens. The results obtained from these experiments are an important benchmark for our research.

The results of the experiments are highly dependent upon the procedures used for the test. It is found that the tissue response were very sensitive to the preparation, handling and testing of the specimen. This has resulted to wide varying range of experimental results. Factors like age of the person the specimen is extracted from, time elapsed between extractions and testing, storage conditions, testing environment, solutions used and loading strain rates for the test play an

important role. A literature review was done to understand the experiments and to study their results.

Hoeltzel *et al* (1992) performed uniaxial tension test on bovine, rabbit and human corneal strips under cyclic loading to understand the behavior of the tissue. They confirmed that the stress and strain relationship were non-linear in nature, with low tangent moduli at small loads and high moduli at higher loads. They also demonstrated the effect of hydration on the sample by measuring the change in dimension under varying the environmental conditions. The specimen shrunk on dry environment and swelled under hydration.

Wollensak *et al* (2003) performed the stress-strain measurement on normal as well as high cross-linked density cornea strips. The specimens were prepared from 5 human corneas that were excised along the superior-inferior direction. The highly crossed linked density cornea strips were obtained by treating the strips with 0.1% Riboflavin solution followed by exposure to Ultraviolet A (UVA) radiation. The UVA treatment induces cross-link, increasing the rigidity of the cornea. Such treatments are successfully used for the treatment of keratoconus, a degenerative eye disease caused by weakening of cornea tissue. The test was performed within 1-2 hours of extraction of the specimen and the result showed 328.9% high stiffness and 4 times high Young's Modulus of treated specimen when compared to the untreated ones.

Elsheikh *et al* (2008) carried out similar uniaxial tensile stress on cornea strips extracted along nasal-temporal (horizontal), superior-inferior (vertical) and diagonal directions. They demonstrated that the specimens obtained along the vertical direction displayed high rigidity compared to the horizontal and diagonal specimens. At low strain rate of 1% per minute, vertical and horizontal specimens had similar stiffness but at high strain rate of 500% per minute vertical specimens were 10% ~ 20% stiffer than the horizontally and diagonally excised specimens.

The measures of stress and strain recorded during the experiments have not been explicitly mentioned in the literature. So, nominal stress and small strain have been assumed when implementing them in the analysis.

2.3.5 Results and Comments

The corneal model developed for the collagen fibrils and matrix was encoded in a custom finite element code. The models were analyzed by varying the pressure from 0 to 400KPa. The nominal stress and strain values were recorded and stress-strain graph was plotted. The analysis was performed for all the three collagen fibril models.

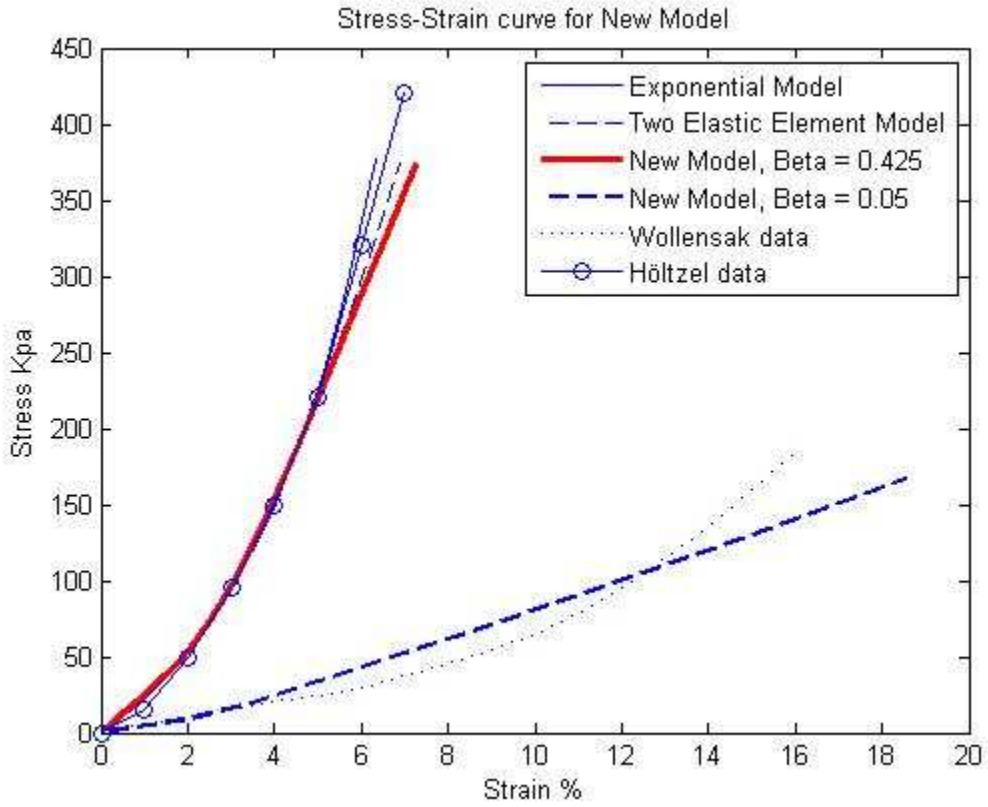

Figure 8: Stress-strain graph fit for the new model.

For the new collagen fibril model, the stress-strain values were tried to fit with the experimental data of Hoeltzel *et al* (1992) and Wollensak *et al* (2003) by varying the cross-link density parameter β. As discussed earlier the experimental stress-strain values highly differed for

each experiment, so we considered two sets of data to compare our result. It is seen from the graph that the model fitted very well with the Hoeltzel's data at β value equal to 0.425. This β value is a reasonable value for cross-link density. Thus our new model resembles the experimental data to a very good degree. This shows that cross-link density parameter plays an important role in describing the response of the collagen fibril.

The model fit with the Wollensak's data at β value equal to 0.05. The fit is not perfect as that obtained for Hoeltzel's data and the β value of 0.05 is very small and does not show any physical sense. This might have resulted due to the experimental procedures carried out to determine the stiffness by the Wollensak, or the tests of the collagen fibrils used to fit the data. The treatments and handling during the experiment might have resulted in loosening the stiffness of the tissue.

The exponential model and the two elastic element model were modified to include the cross-link density by multiplying the equations with the cross-link parameter. The models fit well with the Hoeltzel data at β value equal to 0.425 as shown in Figure 8.

In future investigations, the fibril and tissue model will be used to determine the changes in the mechanical properties for a keratoconic eye by simulation on the entire cornea model. The efficiency of the cross-linking treatment will be studied using such a model.

CHAPTER 3

3.1 Finite Element Modeling of Human Cornea

Finite element models of cornea are very useful tool to study the cornea's mechanical and biological characteristics. They have been extensively used to study the defects and diseases of the eye and also to predict the preoperative and postoperative responses for the refractive surgery.

Pinsky *et al* (2005) developed an anisotropic cornea model based on fibril density function to determine the biomechanical deformation of cornea to study the changes in cornea during and after refractive correction operation. Pandolfi *et al* (2008) created similar model with two preferred orientations of the collagen fibril. They demonstrated the mechanical and optical response of the cornea under varying material properties. Their work emphasizes on dependence on the fibril distribution to create a reliable cornea model. Carvalho *et al* (2009) created a finite element model of the human cornea to understand the biomechanical properties of the cornea for the prediction of keratoconus. The mechanical properties of the cornea like elasticity and rigidity were varied for constant IOP to induce keratoconus in the model. They showed that finite element models can be successfully used to model for the keratoconic eye.

An ideal human cornea model, defines the complex and unique characteristic of the cornea. The reliability of the model is determined by the accurate representation of the collagen matrix, collagen fibril and the architecture of fibril distribution. In this study, an attempt has been made to create a realistic geometric and material model to predict the true mechanical response of the cornea, under the effect of intra-ocular pressure (IOP). Such a model will eventually be used to determine the response of the cornea under the keratoconic conditions. We will determine the degradation of the stiffness of the diseased cornea. The response study will help to

predict the course of the disease. We will then determine how the corneal cross-linking helps the cornea to regain its strength and stiffness and determine the effectiveness of the treatment. The eventual goal is to use this modeling to create a patient-specific treatment regimen using collagen crosslinking.

3.2 Mechanical Properties of Cornea

The cornea exhibits non-linear behavior under the application of IOP. It shows both material and geometrical nonlinearity. The geometric nonlinearity is due to large deformation that is observed in the corneal tissue which will create large error if linear strain theory is considered. The material nonlinearity is due to the non-linear stress-strain response shown by the matrix and collagen fibril. The collagen matrix is represented by a hyperelastic model. The collagen fibrils and its orientation are taken into consideration to determine the biomechanical properties of the cornea. The total response of the cornea is determined by considering strain energy density function as is described in the following sections.

3.3 Modeling of Human Cornea

As discussed in Chapter 1, cornea is made up of 5 layers with the stroma layer comprising 90% of the total cornea thickness. This layer is responsible for providing the great majority of mechanical strength of the tissue (Pandolfi *et al* 2006). Thus, the mechanical response of the cornea can be approximated by only modeling the stroma. Similar approximation has been made by Pandolfi *et al* (2008) and Pinsky *et al* (2005) and the results obtained from their test were fairly accurate with the experimental data.

The cornea material is considered as a heterogeneous, non-linear anisotropic material consisting of incompressible collagen matrix and collagen fibril. The collagen fibrils are considered to be distributed in two preferred direction throughout the cornea. At the center they

are distributed orthogonally in nasal-temporal and inferior-superior directions. At the limbus they are distributed in the circumferential and radial directions. The orthogonal arrangement smoothly transition to the circumferential direction along the transition zone. For computational purpose, the fibrils in the transition zone are linearly interpolated to achieve the desired transformation. Figure 6 shows the approximate distribution of the collagen fibril.

The deformation of the cornea results both rotation and displacement at the limbus which influence the changes in the cornea curvature. The displacement boundary is setup to allow rotation and restrict displacement along the center of the edge of the cornea. Restricting the displacement does not greatly influence the change in curvature (Pandolfi *et al* 2008).

The cornea under physiological conditions is acted upon by the IOP exerted by the aqueous humor behind it. The aqueous humor is the clear gelatinous fluid that fills the space between the lens and the cornea. The IOP is uniformly distributed over the internal surface and is applied perpendicular to the surface. The concept of follower forces is used to calculate the force due to the IOP. Since IOP acts normal to the cornea surface, the direction of the pressure changes as the cornea deforms. To maintain the correct magnitude and direction of the pressure load with respect to the changing surface, follower force is used.

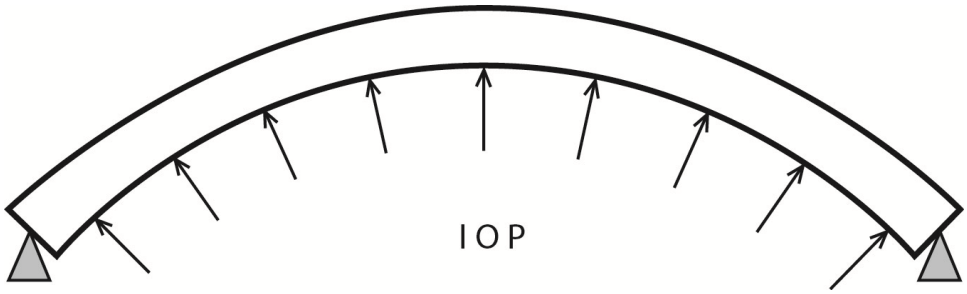

Figure 9: Displacement boundary condition and pressure loading applied in cornea model.

The approach used for creating the cornea tissue model in Chapter 2 has been used for creating the human cornea model. The material model is based on the strain energy density of

collagen fibrils and matrix. We have assumed a continuum finite strain model with material and geometric nonlinearity to describe the mechanism of the human cornea under physiological conditions.

3.3.1 Material model

The response of the cornea to the stress is evaluated by the following strain energy function developed by Pandolfi *et al* (2008)

$$\Psi = U(J) + \overline{\Psi} \tag{13}$$

$$\overline{\Psi}(\overline{\boldsymbol{C}}, \boldsymbol{M}, \boldsymbol{M'}) = \overline{\Psi}_{matrix}(\bar{I}_1) + \overline{\Psi}_{fibril}(\bar{I}_1, \bar{I}_4, \bar{I}_6) \tag{14}$$

where Ψ is the strain energy density of the cornea, $\overline{\Psi}$ is the isochoric response due to the combined strain energy density of collagen matrix, $\overline{\Psi}_{matrix}$ and collagen fibril, $\overline{\Psi}_{fibril}$. *U(J)* is the volumetric response parameter to enforce the incompressibility to the model.

3.3.1.1 Collagen fibrils

The non-linear behavior of collagen fibril is numerically expressed by the strain energy function as defined by Holzaphfel *et al* (2000).

$$\overline{\Psi}_{fibril}(\bar{I}_1, \bar{I}_4, \bar{I}_6) = \sum_{i=4,6} \frac{k_1}{k_2} \{\exp[k_2(\bar{I}_i^* - 1)^2] - 1\} \tag{15}$$

$$I_i^* = \kappa_i \bar{I}_1 + (1 - 3\kappa_i)\bar{I}_i \tag{16}$$

where $\bar{I}_1$ is the first invariant of the modified Right Cauchy-Green Deformation tensor ($\overline{\boldsymbol{C}}$) and $\bar{I}_4$ and $\bar{I}_6$ are its pseudo invariants. The invariants are expressed as follow:

$$\begin{aligned} \bar{I}_1 &= \overline{C}_{II} \\ \bar{I}_4 &= M_I \overline{C}_{IJ} M_J \\ \bar{I}_6 &= M'_I \overline{C}_{IJ} M'_J \end{aligned} \tag{17}$$

The modified Right Cauchy-Green Deformation tensor is the deviatoric part of Right Cauchy-Green Deformation tensor, $\overline{\boldsymbol{C}} = I_3^{-1/3}\boldsymbol{C}$ and $\det\overline{\boldsymbol{C}} = 1$. $\boldsymbol{M}$ and $\boldsymbol{M}'$ are the unit vectors which represent the mean fibril orientation in the two directions as described earlier. $\bar{I}_4$ and $\bar{I}_6$ are the measures of stretch in the $\boldsymbol{M}$ and $\boldsymbol{M}'$ directions respectively. k_1 is a stress like parameter and k_2 is the dimensionless parameter. The values of k_1 and k_2 are determined from mechanical tests.

The dispersion parameter κ_i, defines the distribution of the collagen fibril in the cornea and the parameter introduces anisotropy to the model. The parameter was evaluated at each integration point by using the equation established by Pandolfi *et al* (2008).

$$\kappa_i(\theta) = \left(\frac{\kappa_{i\min} + \kappa_{i\max}}{2}\right) - \left(\frac{\kappa_{i\max} + \kappa_{i\min}}{2}\right)\cos 4\theta \tag{18}$$

$$\kappa_i(\theta,\rho) = \kappa_{i\min} + \frac{1}{2}(\kappa_i(\theta) - \kappa_{i\min})\left(1 - \cos\frac{2\pi\rho}{R_{TZ}}\right) \tag{19}$$

Equation (18) describes the dispersion parameter with respect to angle θ measured from the positive horizontal axis. The κ_i obtained from Equation (18) is used in Equation (19) to obtain new κ_i in terms of the angle θ and radial distance ρ measured from the optical center of the cornea. The values of $\kappa_{i\max} = 0.333$ and $\kappa_{i\min} = 0.133$. These values provide preferred orientation for 60% and dispersion for 40% of the fibril. R_{TZ} is the radius of the transition zone and its value is taken as 1.5mm (Pinsky *et al* 2003).

The Second Piola-Kirchhoff stress for the collagen fibril is evaluated from Equation (15) as follows:

$$\boldsymbol{S}_{fibril} = 2\frac{\partial \overline{\Psi}_{fibril}}{\partial \boldsymbol{C}} = \sum_{i=4,6} 2k_1 \exp(k_2(\bar{I}_i^* - 1)^2)(\bar{I}_i^* - 1)\frac{\partial \bar{I}_i^*}{\partial \boldsymbol{C}} \tag{20}$$

where

$$\begin{aligned}
\frac{\partial \bar{I}_4^*}{\partial \mathbf{C}} &= I_3^{-1/3}\left(\kappa_4(\mathbf{1} - \frac{1}{3}\mathbf{C}^{-1}I_1) + (1-3\kappa_4)(\mathbf{M}\otimes\mathbf{M} - \frac{1}{3}\mathbf{C}^{-1}I_4)\right) \\
\frac{\partial \bar{I}_6^*}{\partial \mathbf{C}} &= I_3^{-1/3}\left(\kappa_6(\mathbf{1} - \frac{1}{3}\mathbf{C}^{-1}I_1) + (1-3\kappa_6)(\mathbf{M}'\otimes\mathbf{M}' - \frac{1}{3}\mathbf{C}^{-1}I_6)\right)
\end{aligned} \tag{21}$$

In equation (21), ***1*** is the second-order identity tensor, i.e. $(\boldsymbol{1})_{AB} = \delta_{\mathbf{AB}}$, where $\delta_{\mathbf{AB}}$ is the Kronecker delta.

The fourth order tangent modulus tensor $\mathbf{C}$ or C_{ABCD}, resulting from above equation is expressed

$$\mathbf{C} = 2\frac{\partial \boldsymbol{S}_{fibril}}{\partial \boldsymbol{C}}$$

$$C_{ABCD} = 4k_1 \sum_{i=4,6} \exp(k_2(\bar{I}_i^* - 1)^2)\left(\left(1 + 2k_2(\bar{I}_i^* - 1)^2\right)\frac{\partial \bar{I}_i^*}{\partial C_{AB}}\frac{\partial \bar{I}_i^*}{\partial C_{CD}} + (\bar{I}_i^* - 1)\frac{\partial^2 \bar{I}_i^*}{\partial C_{AB} C_{CD}}\right) \tag{22}$$

where

$$\frac{\partial^2 \bar{I}_i^*}{\partial C_{AB} C_{CD}} = \kappa_i \frac{\partial^2 \bar{I}_1}{\partial C_{AB}\partial C_{CD}} + (1-3\kappa_i)\frac{\partial^2 \bar{I}_i}{\partial C_{AB}\partial C_{CD}} \tag{23}$$

$$\frac{\partial^2 \bar{I}_1}{\partial C_{AB}\partial C_{CD}} = -\frac{1}{3} I_3^{-1/3}\left(\delta_{AB}C_{CD}^{-1} - \frac{1}{3} I_1 C_{AB}^{-1} C_{CD}^{-1} + C_{AB}^{-1}\delta_{CD} - \mathrm{L}_{ABCD} I_1\right) \tag{24}$$

$$\frac{\partial^2 \bar{I}_4}{\partial C_{AB}\partial C_{CD}} = -\frac{1}{3} I_3^{-1/3}\left(M_A M_B C_{CD}^{-1} - \frac{1}{3} I_4 C_{AB}^{-1} C_{CD}^{-1} + C_{AB}^{-1} M_C M_D - \frac{1}{2}\mathrm{L}_{ABCD} I_4\right) \tag{25}$$

$$\frac{\partial^2 \bar{I}_6}{\partial C_{AB}\partial C_{CD}} = -\frac{1}{3} I_3^{-1/3}\left(M'_A M'_B C_{CD}^{-1} - \frac{1}{3} I_6 C_{AB}^{-1} C_{CD}^{-1} + C_{AB}^{-1} M'_C M'_D - \frac{1}{2}\mathrm{L}_{ABCD} I_6\right) \tag{26}$$

In equation (24), $\mathbf{L}$ or $\mathrm{L}_{ABCD} = \dfrac{\partial C_{AB}^{-1}}{\partial C_{CD}}$.

3.3.1.2 Collagen Matrix

The extrafibrillar matrix is represented by an Incompressible Neo-Hookean Model as

$$\overline{\Psi}_{matrix} = \mu_0 (\bar{I}_1 - 3)/2 \tag{27}$$

The stress and the tangent modulus for the Neo-Hookean model is expressed as follows:

$$\boldsymbol{S}_{matrix} = 2\frac{\partial\overline{\Psi}_{matrix}}{\partial \boldsymbol{C}} = \mu_0 I_3^{-1/3}(\boldsymbol{1} - \frac{1}{3} I_1 \boldsymbol{C}^{-1}) \tag{28}$$

$$\mathbf{C} = 2\frac{\partial \boldsymbol{S}_{matrix}}{\partial \boldsymbol{C}} = \frac{2\mu_0 I_3^{-1/3}}{3}(\frac{I_1}{2}\mathbf{L} + \frac{\mathbf{1}}{\mathbf{3}} I_1 \boldsymbol{C}^{-1} \otimes \boldsymbol{C}^{-1} - \boldsymbol{1} \otimes \boldsymbol{C}^{-1} - \boldsymbol{C}^{-1} \otimes \boldsymbol{1}) \tag{29}$$

The cornea material is considered as an incompressible material. To ensure the incompressibility constraint during deformation, the penalty function *U* is defined. According to Pandolfi *et al* (2008) a suitable penalty function for the corneal model can be represented by

$$U = K \log^2 J \tag{30}$$

where *K* is the penalty parameter and J is the Jacobian, which is the ratio of the volume in the current configuration to the reference configuration. Mathematically $J = \det(\boldsymbol{F})$ and should always be greater than 0 and $\boldsymbol{F}$ is the deformation gradient tensor. Penalty parameter *K* is a deformation independent parameter and is always greater than zero. When the value of *K* is infinity the constraint condition is fully satisfied. Hence, a high value of *K* is desired to satisfy the incompressibility condition, though a value that is too high could lead to an ill-conditioned stiffness matrix. The stress and tangent modulus due to volumetric part is

$$\boldsymbol{S}_{vol} = 2K\boldsymbol{C}^{-1}\log J \tag{31}$$

$$\mathbf{C}_{vol} = 2K(\boldsymbol{C}^{-1} \otimes \boldsymbol{C}^{-1} - \mathbf{L}\log J) \tag{32}$$

The total stress developed in the cornea can now be written as

$$\boldsymbol{S} = \boldsymbol{S}_{vol} + \boldsymbol{S}_{fibril} + \boldsymbol{S}_{matrix} \tag{33}$$

Table 3: Parameter values for the cornea model

Parameter	μ	k_1	k_2	K
Value	60 Kpa	20 Kpa	400	5500 Kpa

Data obtained from Pandolfi et al (2008)

3.3.2 Geometric model

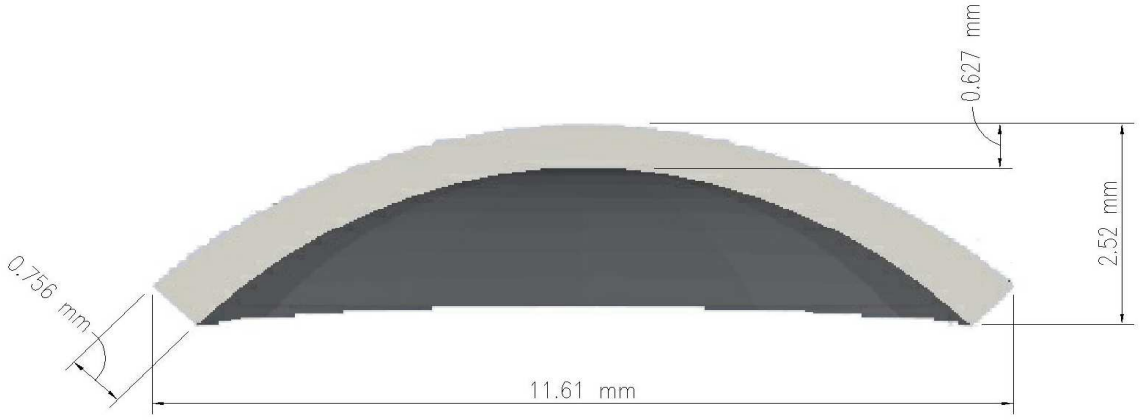

Figure 10: 3-Dimensional finite element model showing the dimensions of the cornea. The outer diameter of the cornea is 11.61mm with thickness of 627 μm at the center and 756 μm at the limbus. The maximum elevation at the apex is 2.52mm.

The cornea has a complex geometrical structure with non-uniform curvature and thickness (Pandolfi *et al* 2006). The interior and exterior surfaces have different radius of curvature. This creates varying thickness in the cornea. It is thinner at the center and thickness towards the edge as shown in Figure 10. Dubbelman *et al* (2006) measured the cornea geometry for the internal and external surfaces of the human cornea. We have used their data for creating our geometric model.

The geometry of the cornea model was meshed into 8-node hexahedral elements by using the parameter based mesh generator developed by Pandolfi *et al* (2006). The mesh was first created in the *x* and *y* plane and is projected onto the *z*-axis to develop a 3-dimensional model. The internal and external surfaces of the cornea are formed by using following biconic surface equation in the cylindrical coordinate system (ρ, θ, z) by the following equation.

$$z(\rho,\theta;R_x,R_y,Q_x,Q_y,\theta_x,z_0) = z_0 - \frac{\rho^2 A}{1+\sqrt{1-\rho^2 B}} \tag{34}$$

where

$$A = \frac{\cos^2(\theta-\theta_x)}{R_x} + \frac{\sin^2(\theta-\theta_x)}{R_y} \tag{35}$$

and $$B = (Q_x + 1)\frac{\cos^2(\theta - \theta_x)}{R_x^2} + (Q_y + 1)\frac{\sin^2(\theta - \theta_x)}{R_y^2} \quad (36)$$

The parameter z_0 is the maximum apical height; R_x and R_y are the maximum curvature of the principal meridian, Q_x and Q_y are the asphericity parameters; and θ_x is the direction of the steepest principal meridian. The values for these parameters are given in Table 4.

Table 4: Parameter used for creating the 3-D model of cornea

Parameters	**External Surface**	**Internal Surface**
$\mathbf{R_x}$	7.71	6.365
$\mathbf{R_y}$	7.87	6.69
$\boldsymbol{\theta_x}$	93 degree	93 degree
$\mathbf{Q_x, Q_y}$	-0.41	-0.52
$\mathbf{z_0}$	2.52	1.891

Data obtained from Dubbelman et al (2006)

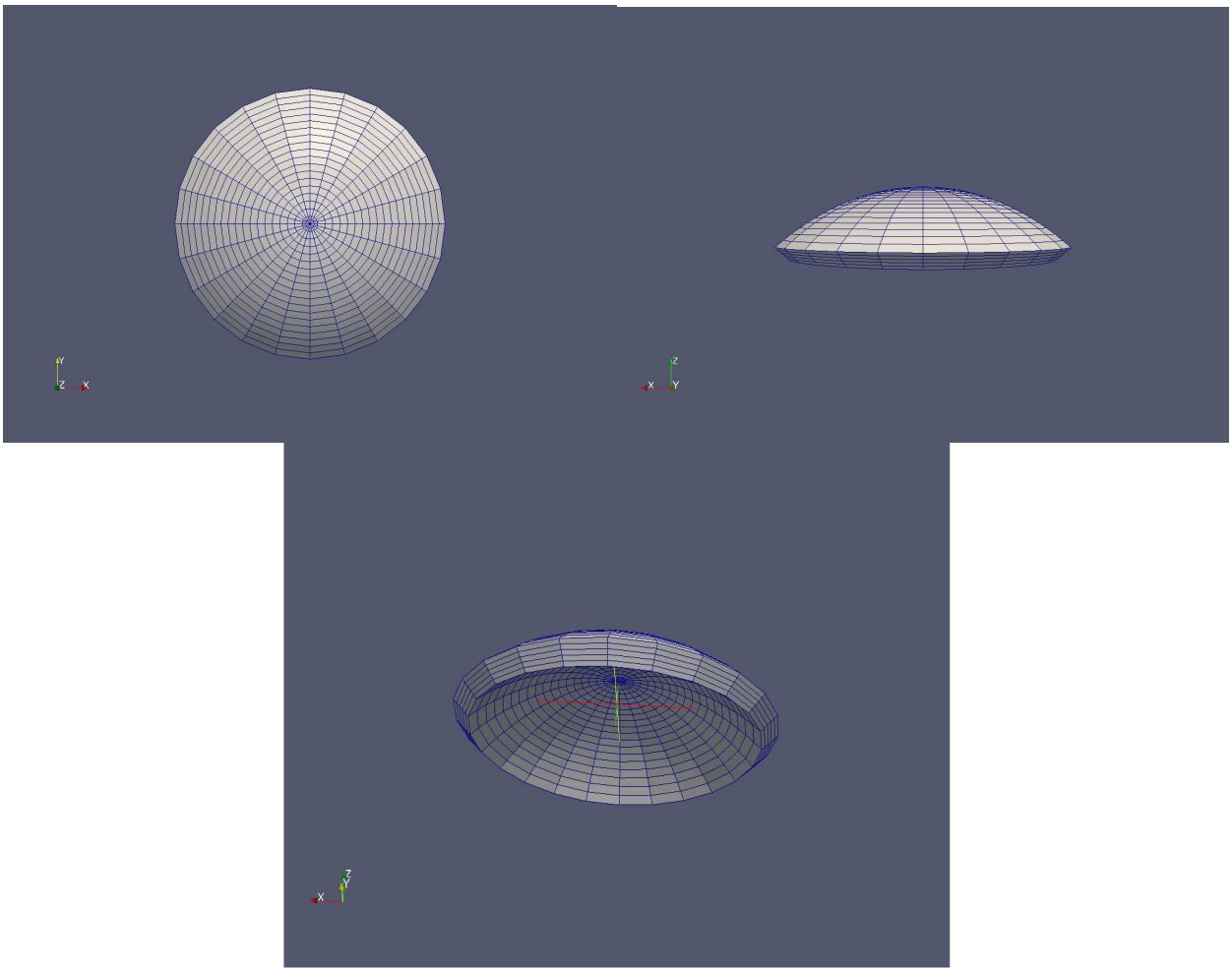

Figure 11: Top view, side view and general view of the 2340 elements meshed human cornea.

3.4 Results and Comments

The cornea model developed in the above section was implemented in a custom finite element code. The algorithm of the code used for the analysis is similar to that described in Chapter 2. The model was analyzed for pressure varying from 0 up to 30 mmHg (slightly above the physiological pressure range of 18 mmHg). The apical displacement values were recorded for the varying pressure values. The graph of the apical displacement versus pressure was plotted for 1170 and 2340 elements. The resulting graph was compared with the laboratory experimental result published by Anderson *et al* (2004) as shown in Figure 12.

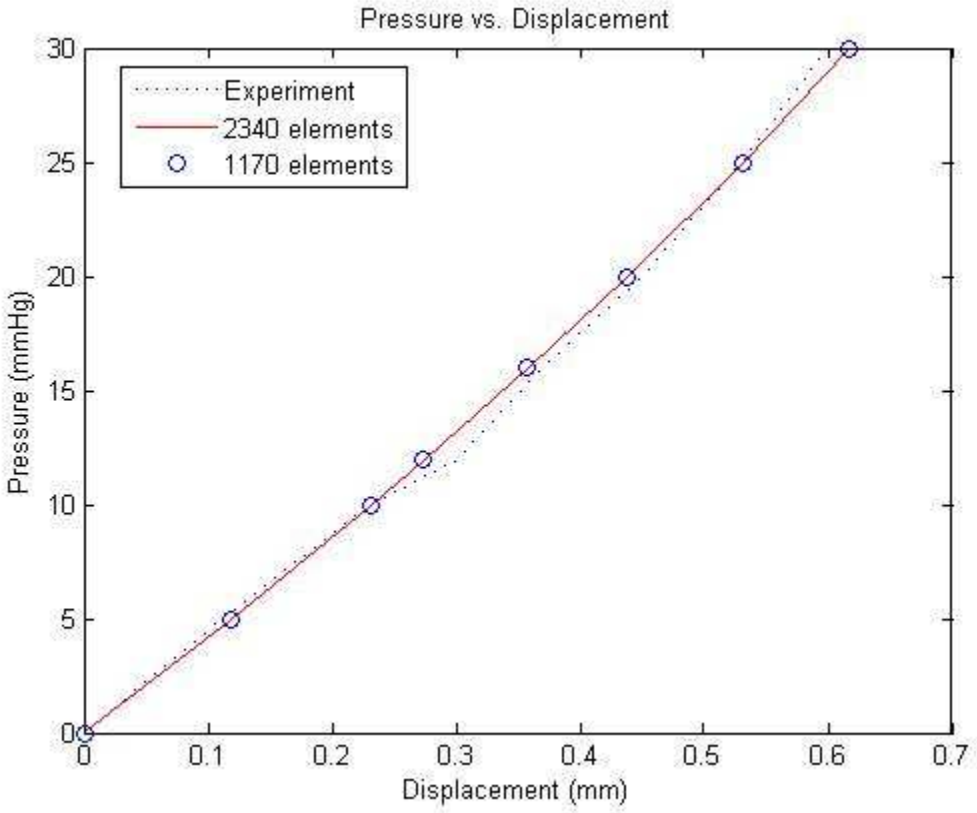

Figure 12: Pressure-Displacement profile for the human cornea

The graph shows that the apical displacement result obtained for the 1170 and 2340 elements are very similar. The error found for the two meshes is 0.06%. We also compared maximum Von Mises stress to check for the convergence of the two meshes. It was seen that

despite the displacement values converged completely the error in the stress was found to be 2.45%, which is considered adequate for this investigation. The stress versus pressure graph for the two meshes is given in Figure 13.

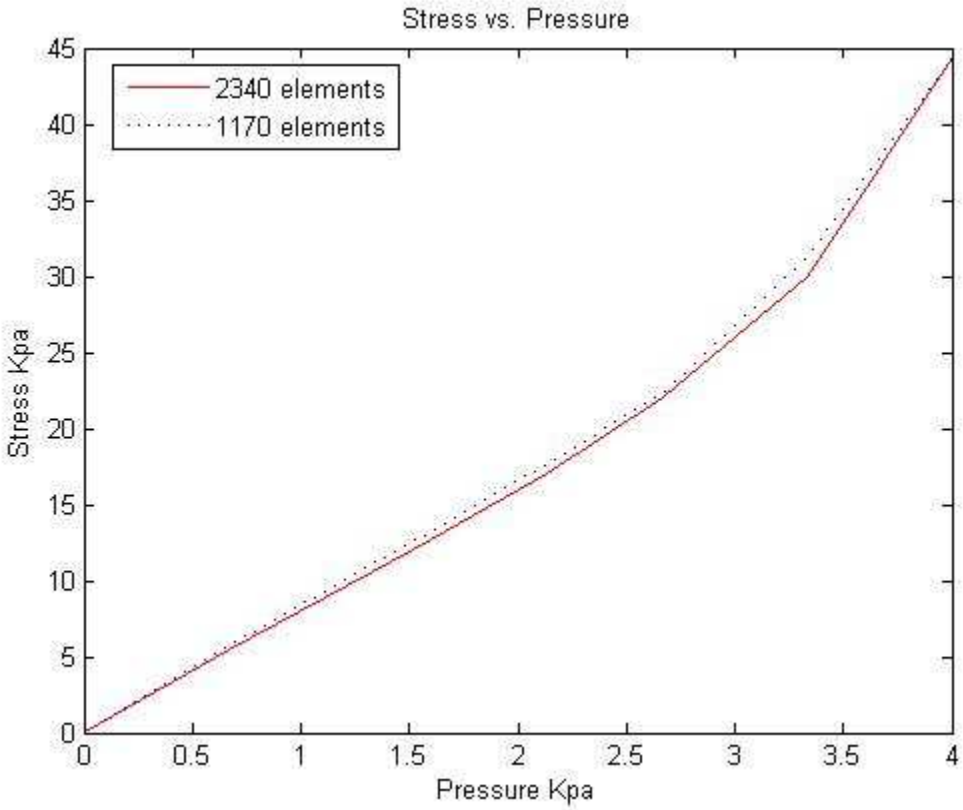

Figure 13: Stress versus pressure for 1170 and 2340 mesh elements showing the convergence of the stress values.

A fairly linear response of the cornea is obtained for the pressure values that we have applied in our model. The simulation results matches very well with the laboratory experimental data. For pressures higher than the physiological IOP we recorded a non-linear response, which is shown in Figure 14.

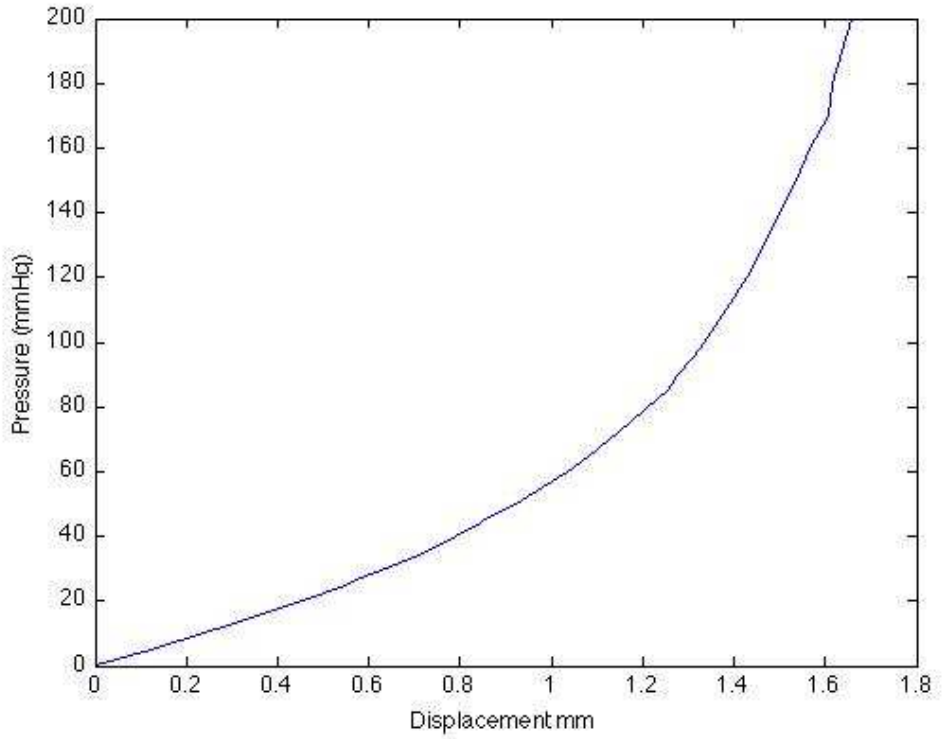

Figure 14: Non-linear response obtained for the cornea model at high IOP.

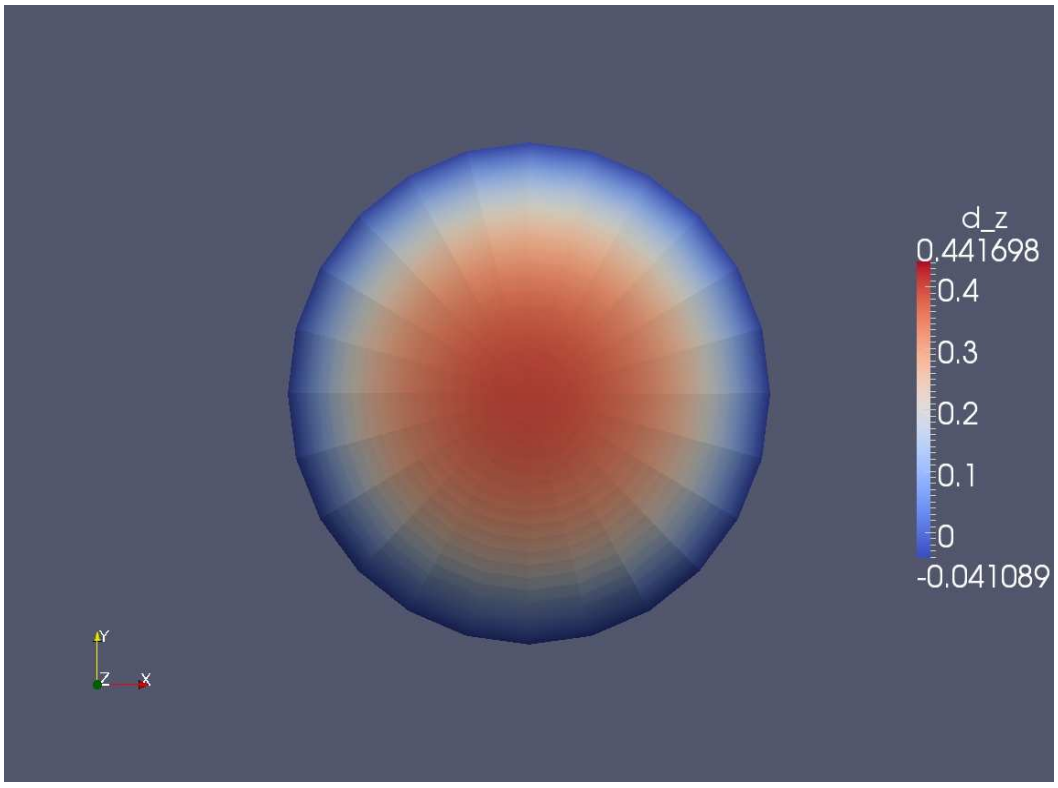

Figure 15: Displacement mapping of the human cornea at 18 mmHg IOP

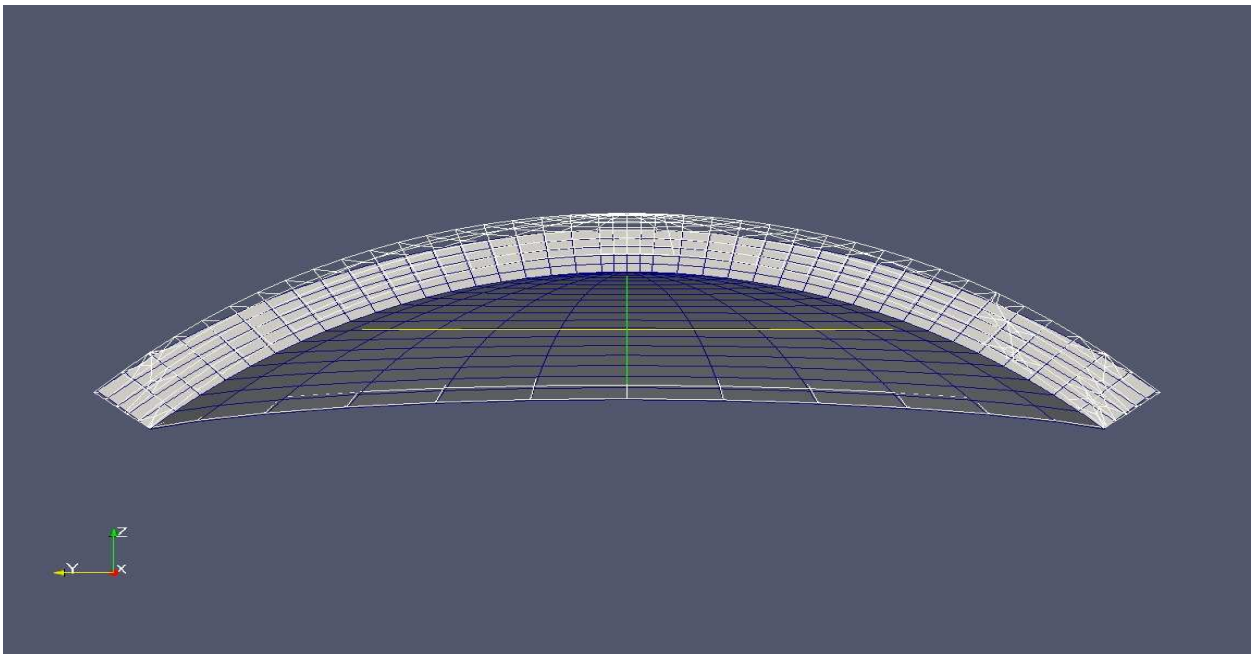

Figure 16: Cross-sectional view of displacement in the cornea. The solid figure shows the original structure and the wire frame figure shows the deformed shape of the corneal due to 18 mmHg of pressure.

The displacement mapping of the cornea is shown in Figure 15. We notice that maximum displacement occurs at the center and it gradually decreases towards the periphery. Figure 16 shows the cross-sectional view of original and deformed shape of the cornea. The solid figure shows the original cornea geometry and the wired frame shows the deformed shape after applying 18 mmHg of pressure.

The stress distribution in the cornea can be obtained for analyzing the results. The stress distribution will be useful to predict the stress concentration over the cornea for later studies of keratoconus eye. Figure 17 shows the Von Mises stress mapping of the cornea.

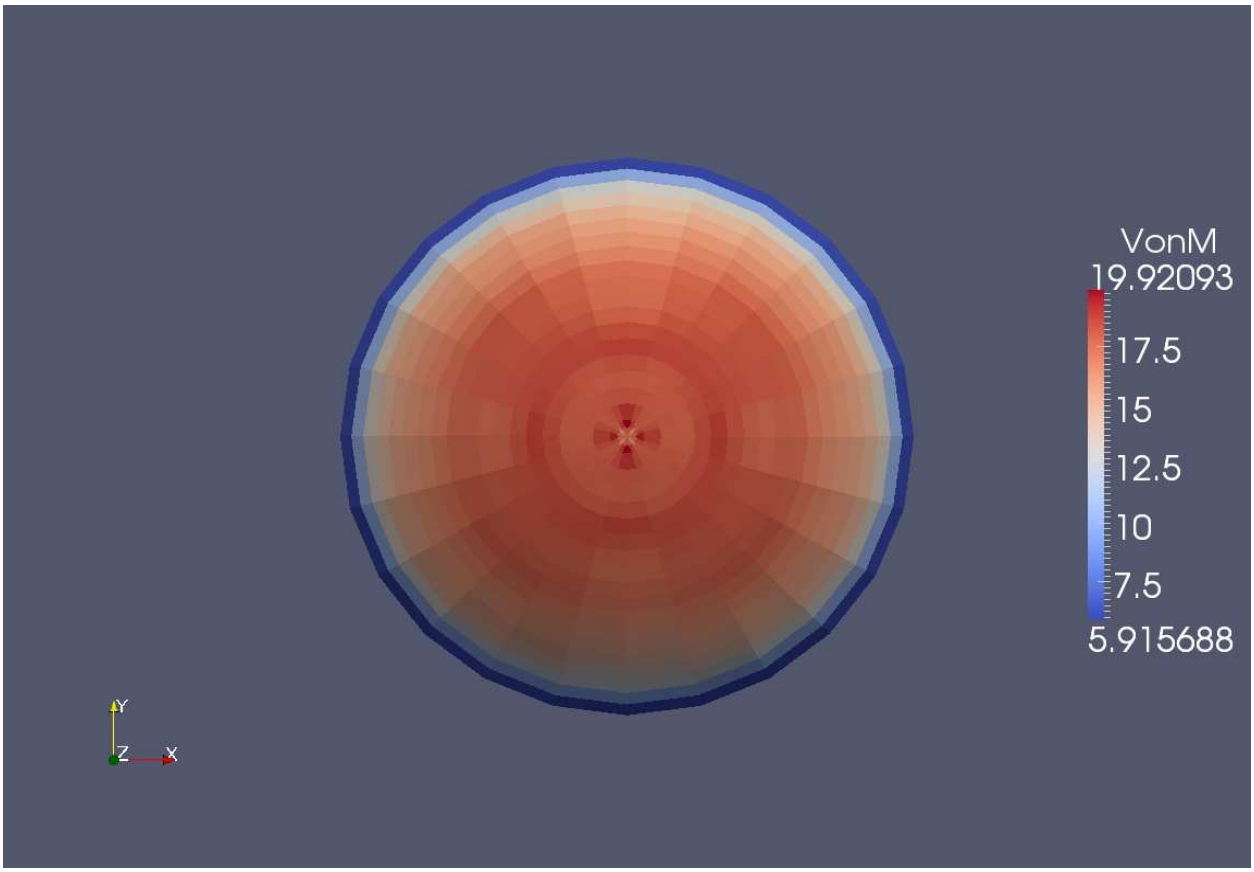

Figure 17: Stress mapping of the cornea.

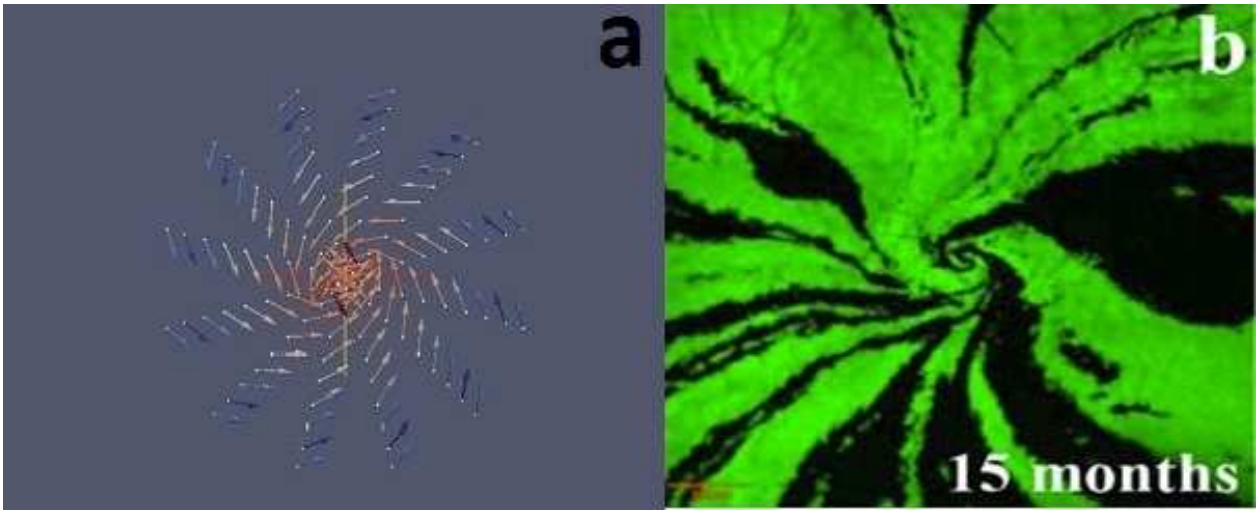

Figure 18: a) Spiral pattern obtained for the cornea model for maximum in plane shear
b) Spiral pattern observed in the rat cornea due to special arrangement of cornea cells

Figure 18a) shows the maximum in plane shear developed in the cornea at 18 mmHg. The shear direction forms a pattern resembling to the whorl pattern observed in the epithelial cells of mouse and rat cornea. These patterns are developed by the special arrangement of the epithelial cells (Boron *et al* 1973, Patel *et al* 2006). The spiral form starts appearing when the mouse reaches 3~6 to 10 weeks old. Figure 18b shows the spiral pattern of a 15-month-old rat. The generation of such patterns in the cornea has not yet been fully understood. This resemblance of the computational result with the dynamic morphogenesis of the eye indicates that the computational model can truly lend insight into the behavior of the cornea. Further studies on the morphogenesis will be carried with the help of the developed model in the future.

A finite element model has been created to replicate the physiological condition of the normal cornea. The results obtained from the analysis shows that the model is able to define the biomechanical properties of the human cornea. The cornea model can now be used to predict the change in the biomechanical properties due to the degradation of the cornea tissue during keratoconus. It can help to understand the disease and to find an efficient treatment to cure and prevent it.

CHAPTER 4

4.1 Conclusion and Comments

The cornea is the medium through which the world is perceived. It is responsible for two thirds of the optical refraction of the eye (Gefen *et al* 2008). The unique transparent nature of the cornea allows light to pass through the eye which makes vision possible. Our study of the cornea is based on understanding the biomechanical response of cornea. The study was carried out in three different hierarchy levels of cornea from fibril, tissue to entire cornea. The multi-scale study helps to understand and correlate the response from the microscopic level to the tissue level. We studied the mechanical properties of collagen fibrils, corneal tissue and the entire cornea and have tried to co-relate them to understand the biomechanical of the cornea.

The non-linear behavior of collagen fibrils was investigated and equations were set up to describe the characteristics of collagen fibril under the application of load. The stress-strain relationship was defined through an exponential equation. The equation formulated by Albanese *et al* 2004 was used and a new equation was also developed based on the physiological response of the collagen fibrils. The three equations were fit with the experimental data using least square regression method and the values of the parameters were determined. The new model fit the experimental data most perfectly with the least error among the three equations, though all fit well.

The equations used to define the collagen fibril were used to create the material model for the corneal tissue. The cornea tissue material was represented by matrix and collagen fibrils. A Neo-Hookean model was used to represent the matrix. The non-linear stress-strain curve was traced for the tissue under tensile loading. The cross-linking parameter β was used to fit the result with the experimental value. The result fit data from Hoeltzel *et al* (1992) for β value equal

to 0.425 very well. This demonstrated a correlation built for the two hierarchy of collagen and also demonstrated the importance of β to the strength of the cornea.

Finally a finite element model of the whole human cornea was simulated. The material and geometric model was created using the model created by Pandolfi *et al* (2008). The matrix was represented by an incompressible Neo-Hookean model. The collagen fibril in the cornea was distributed in two directions with 60% of the fibril along preferential orientation and the remaining 40% with random orientation. The finite element model with 2340 elements was used for the analysis. The result obtained from the analysis showed a non-linear response of the cornea to the IOP. The most interesting part of the result was the ability to observe that maximum in-plane shear strains produce a similar whorl pattern to cells by the biological morphogenesis that can be seen in the cornea.

The integral developed for the evaluation of stress in collagen fibril given by Equation (6) is very complex. It was directly unsolvable and numerically inefficient so it was impractical to use the equation for modeling the whole cornea Thus, we opted for the model used by Pandolfi *et al* (2008) instead of our model.

The next step after creating the finite element model of the cornea will be to fit parameters to the model. The material parameters will be fit using a mathematical algorithm by inputting the loads into a finite element model and attempting to match the recorded deformation obtained from the laboratory.

The geometry measured in the laboratory is of the deformed cornea due to the IOP. So, the unloaded geometry of the cornea will be determined by using an iterative procedure. For this procedure the laboratory scanned geometric data will be taken as the initial guess for the undeformed configuration. A finite element simulation is carried out to determine the resulting

displacement. The displacements are then used to calculate the next assumption, and the process continues until the final loaded configuration matches the unloaded geometry to within a given tolerance. The application of the undeformed configuration for the analysis will improve the accuracy of the result.

The finite element model developed for the normal human cornea can be used to study various complexities of the eye. The model created will be used for studying the keratoconus diseased eye. This disease is caused by the localized weakening of the corneal tissue resulting in vision imperfections. The defect will be induced in the model by varying the mechanical parameters of the cornea at normal IOP. The developed model will be used to calculate the amount of stiffness degradation in the linked fibers due to keratoconus.

Corneal cross-linking is a method to strengthen and stabilize the cornea against keratoconus. The outcomes of this treatment are generally unpredictable. The model will be used to correctly predict the result of the treatment and help to minimize risk associated with it. A quantitative model will be developed to determine the amount of stiffening due to collagen cross-linking and the effect of UVA radiation and riboflavin concentration will also be determined.

The finite element model will be tested by applying specific treatments to cornea and predicting the outcomes in terms of stiffness and deformed shape. Once the model is developed, it can be efficiently used for patient specific cases to optimize the results of the treatment.

List of References

Alastrué, V., Calvo, B., Peña, E. M., and Doblaré, M. (2006), "Biomechanical Modeling of Refractive Corneal Surgery". ASME J. Biomech. Eng., 128, pp. 150–160.

Albanese A., Urso R., Bianciardi L., Rigato M., Battisti E., (2009)," Keratoconus, cross-link-induction, comparison between fitting exponential function and a fitting equation obtained by a mathematical model". Biomedicine & Pharmacotherapy, 63: 693-696.

Anderson, K., El-Sheikh, A., and Newson, T. (2004). "Application of Structura Analysis to the Mechanical Behaviour of the Cornea." J. R. Soc., Interface, 1,pp. 3–15.

Andreassen, T. T., Simonsen, A. H., Oxlund, H. (1980), "Biomechanical properties of keratoconus and normal corneas". Exp Eye Res; 31: 435–44.

Boron, A. J., (1973),"Vortex patterns of the corneal epithelium". Trans Ophthalmol Soc U K 93: 455-472

Buehler, M. J. (2008), "Molecular Nanomechanics of collagen fibrils under varying coss-link densities: atomistic and continuum studies". J. Mech. Behav, Biomed Matter, 1: 59-67

Caravalho L.A., Prado M., Cunha R.H., Neto A.C., Paranhos A., Schor P., Chamon W. (2009), "Keratoconus Prediction using a finite element model of the cornea with local biomechanical properties", Arquivos Brasileiros de Oftamologia, 72(2), 139-145.

Daxer, A., and Fratzl, P. (1997), "Collagen Fibril Orientation in the Human Corneal Stroma and Its Implication in Keratoconus". Invest. Ophthalmol. Visual Sci., 38, pp. 121–129.

Dubbelman, M., Sicam, V. A., and Van der Heijde, G. L. (2006), "The Shape of the Anterior and Posterior Surface of the Aging Human Cornea," Vision Res., 46, pp. 993–1001

Elsheikh. (2008), "Experimental assessment of corneal anisotropy".

Elsheikh, A., and Anderson, K. (2005), "Comparative Study of Corneal Strip Extensometry and Inflation Tests," J. R. Soc., Interface, 2, pp. 177–185.

Eyre DR, Paz MA, Gallop PM. (1984)." Cross-linking in collagen and elastin". Annual Review of Biochemistry, 53: 717-748.

Gefen A., Shalon R., Elad D., Mandel Y. (2009), "Biomechanical analysis of the keratoconic cornea." Journal of the Mechanical Behavior of Biomedical Materials, 2: 224-236.

Graham, J. S., A. N. Vomund, C. L. Philips, and M. Grandbois, (2004), "Structural Change in human type I collagen fibrils investigated by force spectroscopy", Exp. Cell Res. 299: 335-342

Hoeltzel, D. A., Altman, P., Buzard, K., and Choe, K. (1992), "Strip Extensiometry for Comparison of the Mechanical Response of Bovine, Rabbit, and Human Corneas." J. Biomech. Eng., 114, pp. 202–215.

Holzapfel, G. A. (2000), "Nonlinear Solid Mechanics," A Continuum Approach for Engineering. Wiley, Chichester.

Kadler, K. E., Holmes, D. F., Trotter, J. A., Chapman, J. A. (1996),"Collagen fibril formation", Biochem. J. 316, 1-11

Maurice, D. M. (1969), "The Cornea and Sclera," The Eye, 2nd ed., H. Davison, ed., Academic, New York, pp. 489–600.

Meek, K. M., and Newton, R. H. (1999), "Organization of Collagen Fibrils in the Corneal Stroma in Relation to Mechanical Properties and Surgical Practice," J. Refract. Surg., 15, pp. 695–699.

Pandolfi, A., and Manganiello, F., (2006), "A Model for the Human Cornea: Constitutive Formulation and Numerical Analysis," Biomech. Model. Mechanobiol., 5, pp. 237–246.

Pandolfi, A., Holzapfel, G. A., (2008), " Three-dimensional modeling and computational analysis of the human cornea considering distributed collagen fibril orientations." Journal of Biomechanical Engineering, 130(6): 061006.

Pandolfi, A., Fotia, G., and Manganiello, F., (2008), "Finite Element Simulations of Laser Refractive Corneal Surgery," Eng. Comput., in press.

Patel D. V., McGhee C.N., (2006), "Mapping the corneal sub-basal nerve plexus in keratoconus by in vivo laser scanning confocal microscopy", Trans Ophthalmol Vis Sci 47: 1348-1351

Pinsky, P. M., Van der Heide, D., and Chernyak, D., (2005), "Computational Modeling of Mechanical Anisotropy in the Cornea and Sclera," J. Cataract Refractive Surg., 31, pp. 136–145.

Rabinowitz, Y. S., (1998), "Keratoconus", Survery of Ophthalmology, 42(4):297-319.

Sevensson, R. B., Hassenkam, T., Hansen, P., Magnusson, S. P., (2010), "Viscoelastic behavior of discrete human collagen fibrils", J. Mech. Behav. Biomed. Mate, 3: 112-115.

Van der Rijt JAJ, Van der Werf KO, Bennink ML, Dijkstra PJ, Feijen J., (2006), "Micromechanical testing of individual collagen fibrils". Macromolecular Bioscience, 6: 697-702.

Wollensak, G., Spoerl, E., and Seiler, T. (2003), "Stress-Strain Measurements of Human and Porcine Corneas After Riboflavin-Ultraviolet-a-Induced Cross-Linking," J. Cataract Refractive Surg., 29, pp. 1780–1785.

Raiskup-Wolf F. , Hoyer A. , Spoerl, E. , Pillunat, L. E., (2008). "Collagen crosslinking with riboflavin and ultraviolet-A light in keratoconus: Long-term results". Journal of Cataract and Refractive Surgery, 34(5):796–801.

DIPIKA GONGAL, E.I.T

EDUCATION

Master of Science in Civil Engineering (Jan 2012)
University of Illinois at Chicago (UIC), GPA: 4.0/4.0

Bachelor's in Civil Engineering (Dec 2007)
Tribhuvan University, Nepal, GPA: 3.5/4.0

WORK EXPERIENCE

Research Assistant, UIC (Jan 2010 - Current)

- Developed MATLAB code to create 3-dimensional geometric model of human cornea with hexahedral meshing for non-linear finite element analysis
- Created material model of the cornea and implemented it to the finite element model for the analysis
- Developed necessary pressure loading and restraint conditions for analysis to depict the natural condition of the eye, resulting in higher accuracy of the result
- Performed pre-processing, analysis and post-processing jobs of the developed model using MATLAB and Paraview and compared the result with the laboratory data

Teaching Assistant, UIC (Fall 2009 - 2011)

- Assisted professor in managing 50-60 undergraduate and graduate students for the course of 'Finite Element Analysis'
- Tutored students for the course material and assignment problems
- Helped students with ANSYS and MATLAB programming

Civil Engineer, East Consult (P) Ltd, Kathmandu, Nepal (April 2008 - July 2009)

- Performed structural design and cost estimation of residential buildings
- Collaborated with senior bridge design engineer for the design of steel bridges and preparation of engineering drawings of the final design
- Researched on the 'Build Operate Transfer' financing scheme for the infrastructure development projects
- Performed pre-feasibility study for Dakchinkali – Hetauda Bypass road
- Collaborated with Bench Mark (P) Ltd for the transportation impact study and traffic operational analysis for development projects in Portland, Oregon and South Africa
- Wrote technical proposals for various infrastructure projects
- Won the proposal for the 'Planning and Design of Bharatpur Central Bus Terminal' and received funding of 21 Thousand US Dollar from Town Development Fund, Nepal

SPECIAL PROJECT

Undergraduate Final Project: Project Planning and Implementation of Organizational Complex: Bir Hospital Emergency and Trauma Center**,** Kathmandu, Nepal (Aug 2007 - Dec 2007)

- Headed a team for the case study of planning of construction of Bir Hospital Emergency and Trauma Center
- Researched the operational management of the running project which included budget, time schedule and resource management

RELEVANT COURSEWORK

Finite Element Analysis, Non-linear Finite Element Analysis, Structural Dynamics, Plasticity, Computer Aided Analysis of Multibody Systems, Fracture Mechanics I & II, Numerical Methods.

SKILLS

Computer skills: AutoCAD, ANSYS, SAP, MATLAB, MATHCAD, MAPLE, FORTRAN, C++, Microsoft Office (Word, Excel, PowerPoint), Microsoft Project
Language: English, Hindi, Nepali

ACTIVITIES

Member of American Society of Civil Engineers, Engineers' Without Borders and Civil Engineering Students' Society